Evaluating transport in irregular pore networks

Dimitri A. Klimenko,[*] Kamel Hooman, and Alexander Y. Klimenko

School of Mechanical and Mining Engineering, The University of Queensland, QLD 4072, Australia

A general approach for investigating transport phenomena in porous media is presented. This approach has the capacity to represent various kinds of irregularity in porous media without the need for excessive detail or computational effort. The overall method combines a generalized effective medium approximation (EMA) with a macroscopic continuum model in order to derive a transport equation with explicit analytical expressions for the transport coefficients. The proposed form of the EMA is an anisotropic and heterogeneous extension of Kirkpatrick's EMA [Rev. Mod. Phys. **45**, 574 (1973)] which allows the overall model to account for microscopic alterations in connectivity (with the locations of the pores and the orientation and length of the throat) as well as macroscopic variations in transport properties. A comparison to numerical results for randomly generated networks with different properties is given, indicating the potential for this methodology to handle cases that would pose significant difficulties to many other analytical models.

I. INTRODUCTION

There are a large number of applications for both natural and designed porous materials including those in fuel cell technology [1], physiological transport phenomena [2], and heat exchangers [3,4]. By natural porous media, we mean structures with random features, such as irregular pores in view of their sizes and shapes as well as their interconnections. On the other extreme, the term "designed porous media" [5] refers to purposefully constructed porous structures where pores are designed to perform functions under certain constraints, with heat exchanger tube bundles in cross flow as a very good example [6,7]. While porosity can be very high for designed porous materials, natural porous materials typically have much lower values for porosity [5].

Although it is typically the macroscopic transport properties of either a designed or a natural porous medium in which we are interested, these properties are irrevocably tied to the structure of the medium on a microscopic scale. However, due to the complexity of the pore-scale geometry, full analytical results at a microscopic scale are nearly impossible, while numerical simulation tends to be highly computationally intensive and requires excessive detail. The approaches of volume averaging [8] and conditional averaging [9] provide simplified analytical equations, but these equations remain difficult to associate with the microstructure of the porous medium, especially its connectivity.

A convenient approach that allows at least some of these microscopic properties to be accounted for is pore network modeling, which represents the pore space as a large number of pores connected together by narrow throats with simplified geometry for both. With the use of numerical simulations on networks reconstructed from real-world media, realistic predictive estimates of transport coefficients have been made [10,11]. However, such reconstruction processes are relatively difficult, and network simulations can be quite computationally intensive for very large numbers of pores. Analytical models

with suitable averaging remain highly desirable for the purposes of efficiency and robustness.

Unfortunately, there are relatively few analytical approaches to modeling of porous media that take the network microstructure into account. One such approach is the continuous-time random walk (CTRW) method [12–14]; however, apart from some recent efforts [12], the current CTRW formulation usually requires its key parameter to be fitted to experimental data. Another group of approaches is the effective medium approximations (EMAs), which can be applied to stochastic networks, replacing them with deterministic ones on the condition that the average of the local fluctuations must be zero. Typically, an effective medium approximation is applied to a regular network structure [15], and then transport coefficients are calculated by assuming the existence of a smooth macroscopic field, and calculating local fluxes and hence transport coefficients based on this smooth field assumption [16,17]. In general, effective medium approximations are reasonably accurate as long as the medium is not near its percolation limit [18].

The limitations of standard EMAs are demonstrated by network structures reconstructed from three-dimensional (3D) imaging of samples of real-world porous media [10]. It is clear that regular lattices are not representative of the complex, irregular nature of porous media, and although they can often be tuned in order to match empirical data, the parameters in this tuning are typically just fudge factors. In real-world media, the pores and throats vary at macroscopic scales, the throat properties are often anisotropic, and the coordination number exhibits significant variance. Some extensions of the effective medium theory have been proposed that deal with one or two of these issues (anisotropic EMA [19–21], effective throat area [22], variable coordination number [23]), but an effective medium theory which deals with truly irregular networks of the kind we expect from natural porous media seems to be absent from the literature.

In this paper, we propose a generalized single-bond EMA which does not require a recurring network topology, and can have both anisotropy and large-scale variation. This is combined with an explicit derivation of the transport equations

---

*dimitri.klimenko@uqconnect.edu.au

for the effective medium network, in the form of a diffusionlike partial differential equation. Section II describes a general pore-scale model of transport within porous media, in which a porous medium is represented as an irregular pore-throat network which does not conform to any lattice pattern. Pore-scale transport is then modeled using general transport equations based on conservation principles. Section III presents a generalized EMA, which is used to account for microscopic variations due to poor connectivity within the medium. The result of this approximation is a discrete pore network, but one with deterministic throat conductances. Section IV describes the continuum approximation used in order to derive an analytical expression for the transport coefficients in the medium. Section V shows a comparison of the analytical method of Secs. III and IV against numerical simulations for randomly generated pore networks.

II. PORE-SCALE MODEL

In order to achieve a tractable representation of a porous medium at the microscopic level, we begin our analysis with a stochastic pore-throat network model, representing the medium as a network of pores connected together by narrow throats. Although the network model we consider is nonetheless a simplification of the structure of real porous media, we avoid many shortcomings of network models by considering a general class of stochastic networks. Using a stochastic model allows for realistic modeling of porous media by only using the important data about the statistical properties of a medium at a microscopic level, such as types and distributions of connections and pores. The stochastic properties then serve to represent uncertainty about the exact microstructure while taking such information into account. Moreover, the types of networks considered are capable of representing porous media with various kinds of irregularity, including macroscopic heterogeneity, significant variation in coordination numbers, and anisotropy.

Based on a simplification of real media, we consider the pore throats to have negligible storage capacity (typically volume), so that accumulation of the transported quantity occurs within the pores. However, the throats are the primary consideration in determining the throughput within the medium, because overall transport is limited by the constricted nature of the throats. In particular, if there were no throats at all, the medium would consist only of isolated pores, and no transport would take place. As such, transport is primarily modeled within the throats, and at the pore-throat interfaces.

We represent the medium by a network of N pores, which we enumerate with integers $1, \ldots, N$, where N must be large in order for a distinction to emerge between macroscopic and microscopic properties of the medium. A single pore within this network, labeled by its number i, is then described by its location in n-dimensional space, $\boldsymbol{x}_i = (x_i^1, \ldots, x_i^n)$, which we take to be the position of its center, and a vector of additional properties $\boldsymbol{\xi}_i$ (e.g., pore volume). For our purposes, we combine the physical coordinates and the additional properties into the extended vector $\boldsymbol{y}_i = (\boldsymbol{x}_i; \boldsymbol{\xi}_i)$ taking values in some vector space S, which we will call "extended space."

In order to describe the statistical uncertainty that is inherent in modeling the complex and disordered structure of a porous medium, the extended coordinate vectors are considered to be random variables $\boldsymbol{Y}_1, \boldsymbol{Y}_2, \ldots, \boldsymbol{Y}_N$, corresponding to the positions and properties of pores sampled from the medium without replacement. As such, any individual $\boldsymbol{Y}_i$ has an identical marginal PDF (probability density function), $f_Y(\boldsymbol{y})$. For notational convenience, whenever the random variables considered are evident from the arguments, the subscripts will be dropped—e.g., $f(\boldsymbol{y})$ for the single-pore distribution.

Throughout this network, there are throats connecting pairs of pores—these are thin links through which transport between pores can occur. In general, like the pores, these throats could have various properties associated with them. However, for the purposes of the pore-throat network model, these properties are combined into a single value which we call the conductance of the throat, by analogy to electric circuits. For two pores i and j the conductance of a throat connecting them is the value g_{ij}, which describes the ease of transport through the throat—a value of 0 would mean there is no direct link, while a value of ∞ would effectively combine the two pores into a single pore. Moreover, we do not consider the conductance of an individual throat to depend upon the direction of transport, i.e., $g_{ij} = g_{ji}$.

As with the pores, we consider this conductance to be a stochastic variable, G_{ij}, since individual throats in the network could have a variety of values for conductance. It is reasonable to assume that this conductance depends primarily on the properties of the throat itself, and on the pore-throat interfaces on either side. Of course, we can expect correlation between the throat and pore properties—for example, larger pores would generally have larger throats. With this in mind, we express the distribution for conductances for any given throat by

$$f_{G_{ij}}(g) = f(g \mid \boldsymbol{y}_i, \boldsymbol{y}_j), \tag{1}$$

which accounts for the effect of pore properties and locations on the throat conductance, as well as for independent randomness within the throats themselves. It is important to note that throat length is also accounted for in this representation, since the physical coordinates of the pores are included in $\boldsymbol{y}_i$ and $\boldsymbol{y}_j$.

In a realistic porous medium, it is clear that the vast majority of pairs of pores do not have any throat connecting them at all, especially when the pores are spatially distant. Considering this, we let $\Psi(\boldsymbol{y}_i, \boldsymbol{y}_j)$ be the probability that a throat between pores with extended coordinates $\boldsymbol{y}_i, \boldsymbol{y}_j$ is present, and so the conductance distribution for the throat can be written as

$$f(g \mid \boldsymbol{y}_i, \boldsymbol{y}_j) = \Psi(\boldsymbol{y}_i, \boldsymbol{y}_j) f^*(g \mid \boldsymbol{y}_i, \boldsymbol{y}_j)$$
$$+ [1 - \Psi(\boldsymbol{y}_i, \boldsymbol{y}_j)] \delta(g), \tag{2}$$

where f^* is the distribution over nonzero values of conductance (i.e., conditional upon $G > 0$), and δ is the Dirac δ function.

This stochastic network model is a very general type of random graph, with the addition of random edge weights—the conductance values representing the transport properties of the throats. Of the many classes of random graphs studied in the literature, the closest well-known one is the random geometric graph [24] due to the spatial nature of the node parameters and localized connectivity. Another approach is fitness-based connectivity [25], but this concept is targeted

towards the generation of scale-free networks and hence is not used here.

Having defined the throat conductance, we can derive a general transport equation valid for a variety of different transport phenomena, including diffusion, conduction heat transfer, flow of electrical current, transport across biological membranes, and linear cases of fluid flow (e.g., incompressible Newtonian Stokes flow). We consider interpore transport to be driven by a "potential difference" between two pores, while the transport phenomenon represents the tendency for these potentials to equilibrate.

In this paper, we will use the terminology of molecular diffusion, and so we identify the potential of a pore as the concentration of the substance within the pore, $c_i = m_i/V_i$, where m_i is the amount of the substance in the pore, and V_i is the volume of the pore. There is a net flow of particles from pores with higher concentrations to those with lower concentrations, resulting in a flow rate through any given throat (from pore i to pore j) defined by

$$q_{ij} = -q_{ji} = g_{ij}(c_i - c_j). \qquad (3)$$

With the use of a conservation law within the ith pore, we can finally derive the *master equation*,

$$\frac{dm_i}{dt} = \sum_{j=1}^{N} q_{ji} = \sum_{j=1}^{N} g_{ij}(c_j - c_i), \qquad (4)$$

which is a system of N differential equations that describes transport within the medium at the pore scale. As noted previously, this equation is applicable to a wide range of transport processes; expressions for throat conductance g in terms of the geometric properties of the throat and the properties of the materials or substances involved are given in Appendix A for several of these transport phenomena.

III. NONUNIFORM EFFECTIVE MEDIUM APPROXIMATION

If the porous medium is very well connected, global transport can be directly approximated using the continuum approximation described in Sec. IV using the mean or expected value for the conductance of each throat,

$$\bar{g}(\mathbf{y}_i, \mathbf{y}_j) = \int_0^\infty g f(g|\mathbf{y}_i, \mathbf{y}_j) \, dg. \qquad (5)$$

However, in general, the media we consider do not meet this requirement. In order to resolve this, we apply a nonuniform effective medium approximation that transforms networks with intermittent throats or significant variations in conductance into well-connected ones.

The importance of connectedness within a pore network is highlighted by many results in the area of percolation theory [26]. In particular, a very general result for such systems is that in the limit $N \to \infty$, there is a critical level of connectedness for the system which is called the "percolation threshold"—below this level, the overall network collapses into small, disjoint clusters, and hence there is no transport at the macroscopic level [27].

In general, it is extremely difficult to derive the percolation threshold, or transport behavior in the vicinity of the threshold, for all but the simplest of network structures. This is especially pertinent to the proposed network model, since it has an irregular structure and correlations between the pores and throats. However, a simple analysis of the proposed model can identify some important structural properties. Using Ψ, the probability that a throat is present, we can derive the expected coordination number of a pore with extended coordinates $\mathbf{y}$ as [25]

$$z(\mathbf{y}) = (N-1) \int_S f(\mathbf{y}^\circ) \Psi(\mathbf{y}, \mathbf{y}^\circ) d\mathbf{y}^\circ. \qquad (6)$$

The value of z is crucial to overall transport in the medium—if this value is high, the network is well connected and using the mean conductance for every bond should prove to be a reasonable approximation. Unlike with N, we cannot simply assume that z is large—pore networks extracted from 3D images of various porous media [10,28–32] have usually had average coordination numbers between 2 and 7.

To illustrate the effects of low values of z, consider the simple case of a regular lattice pattern, in which every throat independently has probability p of being present ($g = g_0$) and probability $1 - p$ of being absent ($g = 0$). Using a single-bond EMA, Kirkpatrick [15] has shown that the global transport properties of such a network are roughly the same as those of an identical lattice pattern in which every throat is present, with conductance [33]

$$\tilde{g} = g_0 p \frac{z-2}{z-2p}. \qquad (7)$$

As $p \to 1$ or $z \to \infty$, Eq. (7) approaches the mean value approximation, $\bar{g} = g_0 p$. However, in cases where p and z are small, it is clear that the mean value approximation is wrong by a significant margin, and hence a better approximation is required.

Unfortunately, in general, single-bond EMA cannot account for behavior near the percolation threshold of the system, because of a failure to account for the effects of correlations between the throats in the system [18]—in the terminology of percolation theory, the correlation length of the system diverges at the threshold [27]. Nonetheless, the accuracy of EMA tends to be quite good for systems that are not in the vicinity of their percolation thresholds [18]. For the treatment of cases where z is small, with significant stochastic variation in the throats (especially when there is a high probability of absence), we apply a generalization of single-bond EMA in which the bond conductances are not uniform, but instead vary depending on the extended coordinates of the pores they connect. The result of this approach is the transforming the probabilistic conductances g_{ij} into deterministic effective values $\tilde{g}_{ij}$.

Unlike Kirkpatrick's approach for the regular lattice, we do not consider the effective conductance to be equal for every throat; instead, we account for the dependence of a throat's properties on the properties and locations of the pores it connects. Consequently, we solve for an an unknown function $\tilde{g}_{ij} = \tilde{g}(\mathbf{y}_i, \mathbf{y}_j)$—effective throat conductance as a function of pore locations and attributes, creating an effective medium which is heterogeneous and anisotropic in nature. Note that the resulting effective medium is continuous in some sense—the

pores are effectively smeared out over their distributions, and the throat conductances are described by a function $\tilde{g}$.

Although for regular lattices the effective medium can have low average coordination numbers, the randomness in pore properties and locations in the proposed model means that in our case the effective medium must usually have both large N and a large coordination number $\tilde{z}$ in order to properly eliminate the local fluctuations in the original network. In terms of the original network, the value $\tilde{z}$ is the number of pores in what we call the *locale* of pore i—that is, the region of the medium to which pore i can (with nonzero probability) have direct connections. Fortunately, the structure of real-world porous media is generally in line with this assumption—direct connections tend to occur only between nearby pores, but there are generally many other pores in the vicinity of any given pore.

In order for the approximation proposed in this paper to be valid, the overall statistical properties of the medium [i.e., the distributions $f(\boldsymbol{y})$ and $f(g \mid \boldsymbol{y}_1, \boldsymbol{y}_2)$] must not change significantly within a single locale. This type of assumption is typically almost inevitable in the derivation of a continuum model, although here it is only required on relatively small scales and so we can still account for macroscopic heterogeneity such as spatial variation in composition, structure, or porosity. Aspects of the pores such as pore size can also be included in these statistical properties, but it is important to note that in such a case the locale consists of pores of varying sizes, and sharp changes in throat statistics between connected pores are allowed only with negligible frequency. In real-world porous media with fractal properties (coal may serve as a notable example) this type of approach should be entirely reasonable [9,34]; in such cases, we expect transport to occur via a cascade process in which flow between large pores and much smaller ones occurs primarily via pores of intermediate size.

The self-consistent condition of effective medium theory states that the fluctuations over a section of the original stochastic network, compared to its replacement in the effective medium, must average to zero. In our case, we consider this condition when applied to a single throat within the network connecting pores with extended coordinates taking the fixed values $\boldsymbol{y}_i$ and $\boldsymbol{y}_j$; analogously to Kirkpatrick [15], we express this condition as

$$\int_0^\infty f(g \mid \boldsymbol{y}_i, \boldsymbol{y}_j) \frac{g - \tilde{g}(\boldsymbol{y}_i, \boldsymbol{y}_j)}{g + \tilde{h}(\boldsymbol{y}_i, \boldsymbol{y}_j)} \, dg = 0, \quad (8)$$

where $\tilde{h}(\boldsymbol{y}_i, \boldsymbol{y}_j)$ is the expected two-point conductance between pores at positions $\boldsymbol{y}_i$ and $\boldsymbol{y}_j$, in the absence of a throat directly connecting them—this is the net flow through the network resulting from externally forcing a unit difference in concentration between those pores. This two-point conductance is usually defined in terms of Green's functions [35]; a detailed discussion with exact values for many infinite regular lattices can be seen in [36]. This equation allows the throat conductance to vary with the locations of the pores and the orientation and length of the throat, resulting in a heterogeneous and anisotropic effective medium. With this in mind, we term this approach the *nonuniform effective medium approximation* (NEMA). In its most general form, Eq. (8) is very difficult to solve, since the values for $\tilde{h}$ between any two pores depends on every other throat in the effective medium,

and consequently on the values of the function $\tilde{g}$, while $\tilde{g}$ in turn depends upon $\tilde{h}$. However, under certain conditions, we can derive approximations for $\tilde{g}$ and $\tilde{h}$ which make the problem much more tractable.

As long as almost all bonds in the original network have a very low probability of being present, $\Psi \ll 1$, which naturally results in $z \ll \tilde{z}$ and consequently (as needed) a well-connected effective medium, we can approximate $\tilde{g}$ by

$$\tilde{g}(\boldsymbol{y}_i, \boldsymbol{y}_j) = \int_0^\infty \frac{f(g \mid \boldsymbol{y}_i, \boldsymbol{y}_j)}{1/g + 1/\tilde{h}(\boldsymbol{y}_i, \boldsymbol{y}_j)} \, dg. \quad (9)$$

For natural porous media, the assumption of $\Psi \ll 1$ should prove to be a reasonable one, as there tend to be many pores in the vicinity of any given pore, but relatively few of these tend to be directly connected. For the details of the derivation of Eq. (9), see Appendix B.

It is clear that as long as an expression for the unknown function $\tilde{h}(\boldsymbol{y}_i, \boldsymbol{y}_j)$ can be determined, Eq. (9) specifies the values of the conductances in the effective medium. Fortunately, the value of $\tilde{h}$ is only important within a pore's locale, since long throats should be very unlikely and have very low conductances, resulting in negligible values of $\tilde{g}$ from Eq. (9) regardless of $\tilde{h}$. Since the effective medium must have a large coordination number, we can see that in general $\tilde{h} \gg \tilde{g}$ and so the presence or absence of a direct connection is insignificant for calculating $\tilde{h}$.

To approximate the conductance between pore i and pore j, we consider it to consist of three conductances in series—two input conductances from the pores into their locales, which we represent by the unknown function $\tilde{h}_{\text{in}}(\boldsymbol{y})$, and a third term which comes from the interconnection between these locales.

For neighboring pores, we expect that in a porous medium the locales of these pores should overlap significantly [37], resulting in $O(\tilde{z}^2)$ connections to one another, causing the third term to be negligible in comparison with the input conductances. This gives

$$\tilde{h}(\boldsymbol{y}_i, \boldsymbol{y}_j) \approx \frac{1}{1/\tilde{h}_{\text{in}}(\boldsymbol{y}_i) + 1/\tilde{h}_{\text{in}}(\boldsymbol{y}_j)}, \quad (10)$$

where we approximate $\tilde{h}_{\text{in}}$ through connections of each pore to the distribution of other pores in the effective medium, i.e.,

$$\tilde{h}_{\text{in}}(\boldsymbol{y}) = (N - 1) \int_S f(\boldsymbol{y}^\circ) \tilde{g}(\boldsymbol{y}, \boldsymbol{y}^\circ) \, d\boldsymbol{y}^\circ, \quad (11)$$

whereas integration occurs over values of $\boldsymbol{y}^\circ$ in the extended space, with corresponding volume element $d\boldsymbol{y}^\circ$.

By substituting Eq. (10) into Eq. (9) and the result into Eq. (11), and dividing both sides by $\tilde{h}_{\text{in}}(\boldsymbol{y})$, we get

$$1 = \int_S \int_0^\infty \frac{(N - 1) f(g, \boldsymbol{y}^\circ \mid \boldsymbol{y})}{1 + \tilde{h}_{\text{in}}(\boldsymbol{y})[1/g + 1/\tilde{h}_{\text{in}}(\boldsymbol{y}^\circ)]} \, dg \, d\boldsymbol{y}^\circ. \quad (12)$$

This equation implicitly defines the function $\tilde{h}_{\text{in}}(\boldsymbol{y})$, which can then be used in Eqs. (10) and (9) to determine the values of $\tilde{g}$ within the effective medium.

Using the previous assumption that the distribution for conductances and properties does not change significantly within a given locale, and since $\tilde{h}_{\text{in}}$ primarily depends on the values of $\tilde{g}$, it follows that for $\boldsymbol{y}^\circ$ within the locale of $\boldsymbol{y}$, $\tilde{h}_{\text{in}}(\boldsymbol{y}^\circ) \approx \tilde{h}_{\text{in}}(\boldsymbol{y})$. With this approximation, the denominator of

the integral becomes independent of $\boldsymbol{y}^{\circ}$; in conjunction with Fubini's theorem this gives

$$\frac{1}{N-1} = \int_0^{\infty} \frac{1}{2 + \tilde{h}_{\text{in}}(\boldsymbol{y})/g} \int_S f(g, \boldsymbol{y}^{\circ} \mid \boldsymbol{y}) \, d\boldsymbol{y}^{\circ} \, dg. \quad (13)$$

The inner integral evaluates to the distribution of conductances coming out of a single pore with extended coordinates $\boldsymbol{y}$, i.e.,

$$f(g \mid \boldsymbol{y}) = \int_S f(g, \boldsymbol{y}^{\circ} \mid \boldsymbol{y}) \, d\boldsymbol{y}^{\circ}, \quad (14)$$

resulting in

$$\frac{1}{N-1} = \int_0^{\infty} \frac{f(g \mid \boldsymbol{y})}{2 + \tilde{h}_{\text{in}}(\boldsymbol{y})/g} \, dg. \quad (15)$$

This gives the value of $\tilde{h}_{\text{in}}$ for any $\boldsymbol{y}$, which, together with Eqs. (10) and (9), specifies the throat conductances within the effective medium.

IV. CONTINUUM APPROXIMATION

A. Reduced master equation

Applying the EMA described in the previous section accounts for the stochastic variation in throat conductances in the original network. However, this still leaves a system with an equation for each individual pore, i.e.,

$$\frac{dm_i}{dt} = \sum_j \tilde{g}_{ij}(c_j - c_i), \quad (16)$$

which is merely the master equation (4) but applied to the effective medium rather than to the original random network. In order to simplify this equation, we wish to transform it into a continuous form, wherein the amount of substance m and concentration c are considered over the extended space rather than within individual pores. This is achieved by considering the ensemble of realizations of the pore positions and properties in the effective medium, and then converting to continuous form by taking the limit of a summation over discrete regions.

Assume that the extended space S is partitioned into countably many regions S_I (for $I \in \mathbb{N}$) such that each S_I is a neighborhood of some point in extended space, $\boldsymbol{y}_I$. Here we mean "partition" in the usual mathematical sense, i.e., that the regions S_I must be pairwise disjoint and cover S. If we let A_I be the set of pores contained within S_I, i.e., $A_I = \{i \mid \boldsymbol{y}_i \in S_I\}$, it follows that, in turn, the sets A_I form a partition of the set of all pores, $A = \{1, \dots, N\}$.

The total amount of substance within the region S_I is given by

$$M_I = \sum_{i \in A_I} m_i, \quad (17)$$

and so, applying Eq. (4), the transport equation for M_I in the effective medium is given by

$$\frac{dM_I}{dt} = \sum_{i \in A_I} \sum_{J \in \mathbb{N}} \sum_{j \in A_J} \tilde{g}_{ij}(c_j - c_i). \quad (18)$$

Since $\tilde{g}_{ij} = \tilde{g}(\boldsymbol{y}_i, \boldsymbol{y}_j)$, and the S_I are neighborhoods in extended space, it follows that as long as they can be made sufficiently small, with $\tilde{g}$ continuous over each region (i.e., the

set of discontinuities of $\tilde{g}$ must have measure zero), then for any $i \in A_I$, $j \in A_J$ we have

$$\tilde{g}_{ij} = \tilde{g}(\boldsymbol{y}_I, \boldsymbol{y}_J). \quad (19)$$

Since the value of the sum in Eq. (18) is finite, we can change the order of summation. If we denote the number of pores in the region S_I by N_I, then Eq. (18) becomes

$$\frac{dM_I}{dt} = \sum_{J \in \mathbb{N}} \tilde{g}(\boldsymbol{y}_I, \boldsymbol{y}_J) \left(N_I \sum_{j \in A_J} c_j - N_J \sum_{i \in A_i} c_i \right). \quad (20)$$

As long as either (1) all pores have equivalent volume, V_0, or (2) the volume is included as a coordinate of the extended space (in which case we can set $\xi_i^1 = \ln V_i$ without loss of generality), the volume of each pore in a region can be considered equal, i.e., $V_i = V_I$. We now introduce averaged concentrations within each region,

$$C_I = \frac{M_I}{N_I V_I} = \frac{1}{N_I} \sum_{i \in A_I} c_i. \quad (21)$$

It is important to note that these concentrations are based on the total pore volume in each region, not the volume of physical space in each region. With these concentrations, we can now write the master equation in terms of the regions,

$$\frac{dM_I}{dt} = \sum_{J \in \mathbb{N}} \tilde{g}(\boldsymbol{y}_I, \boldsymbol{y}_J) N_I N_J (C_J - C_I). \quad (22)$$

If we now consider the pores as being probabilistically spread over the space, the quantities N_I become the expected number of pores in each region. These can be approximated using the marginal distribution $f(\boldsymbol{y})$ as

$$N_I = N \int_{S_I} f(\boldsymbol{y}) d\boldsymbol{y}. \quad (23)$$

If we also let the regions become infinitesimal, we get the *reduced master equation*,

$$\frac{\partial M}{\partial t}(\boldsymbol{y}, t) = N^2 \int_S \tilde{g}(\boldsymbol{y}, \boldsymbol{y}^{\circ}) f(\boldsymbol{y}) f(\boldsymbol{y}^{\circ})$$
$$\times [C(\boldsymbol{y}^{\circ}, t) - C(\boldsymbol{y}, t)] \, d\boldsymbol{y}^{\circ}, \quad (24)$$

where C is the local concentration of the substance per unit pore volume, and M is the local concentration of the substance per unit of extended spatial volume.

B. Diffusional approximation

In principle, the reduced master equation can be solved directly, but a simplified form is still desirable. Fortunately, we know from Sec. III that for any given $\boldsymbol{y}$, $\tilde{g}$ vanishes outside its locale, while the functions $\tilde{g}$ and f must not change significantly within this locale. Based on this, we expect C to behave similarly, and so we use power series to derive an approximation for Eq. (24) in the form of a diffusionlike partial differential equation.

We introduce $\Delta \boldsymbol{y} = \boldsymbol{y}^{\circ} - \boldsymbol{y} = (\Delta y^1, \Delta y^2, \dots)$, and let $\tilde{g}_2$ satisfy

$$\tilde{g}(\boldsymbol{y}, \boldsymbol{y}^{\circ}) = \tilde{g}_2(\boldsymbol{y} - \boldsymbol{y}^{\circ}, \boldsymbol{y} + \boldsymbol{y}^{\circ}) = \tilde{g}_2(\Delta \boldsymbol{y}, 2\boldsymbol{y} + \Delta \boldsymbol{y}). \quad (25)$$

Notably, since $\tilde{g}$ is symmetric, it follows that $\tilde{g}_2$ must be an even function with respect to its first argument, $\Delta \boldsymbol{y}$. The

introduction of $\tilde{g}_2$ allows us to rewrite the reduced master equation as

$$\frac{\partial M}{\partial t} = N^2 \int_S \tilde{g}_2(\Delta \mathbf{y}, \mathbf{y} + \Delta \mathbf{y}) f(\mathbf{y}) f(\mathbf{y} + \Delta \mathbf{y})$$
$$\times [C(\mathbf{y} + \Delta \mathbf{y}, t) - C(\mathbf{y}, t)] \, d(\Delta \mathbf{y}). \qquad (26)$$

Taking power series expansions for $\tilde{g}_2(\Delta \mathbf{y}, \mathbf{y} + \Delta \mathbf{y})$, $f(\mathbf{y} + \Delta \mathbf{y})$, and $C(\mathbf{y} + \Delta \mathbf{y}, t) - C(\mathbf{y}, t)$ yields a diffusional approximation—for details on this derivation, see Appendix C. Here we introduce

$$\phi(\mathbf{y}) = N f(\mathbf{y}) V(\mathbf{y}), \qquad (27)$$

which means that $M(\mathbf{y}) = \phi(\mathbf{y}) C(\mathbf{y})$. In the case where there are three spatial dimensions and no additional properties, i.e., $\mathbf{y} = (x^1, x^2, x^3)$, ϕ is in fact the local (averaged) porosity of the medium. If ϕ does not depend on time, then (using the Einstein summation convention over Greek indices) the final equation takes the form

$$\phi(\mathbf{y}) \frac{\partial C}{\partial t} = \frac{\partial}{\partial y^\alpha} \left[\phi(\mathbf{y}) D^{\alpha\beta}(\mathbf{y}) \frac{\partial C}{\partial y^\beta} \right], \qquad (28)$$

where the elements of the diffusion tensor D are given by

$$D^{\alpha\beta}(\mathbf{y}) = \frac{N f(\mathbf{y})}{2 V(\mathbf{y})} \int_S \Delta y^\alpha \Delta y^\beta \tilde{g}_2(\Delta \mathbf{y}, 2\mathbf{y}) \, d(\Delta \mathbf{y}). \qquad (29)$$

It is important to note that while C is not conserved, Eq. (28) is conservative with respect to $M = \phi C$, as should be the case for transport with no sources or sinks. The above integral is assumed to converge; any case where it does not would likely be a case of anomalous diffusion, which cannot be represented by the above equations. It can be seen that this equation takes a form very similar to the Fokker-Planck (Kolmogorov forward) equation, which governs the PDF of an Itō-type random walk. However, the Kolmogorov forward equation differs in that the diffusion coefficient is differentiated twice with respect to $\mathbf{y}$.

V. RESULTS

In this section, the accuracy of the approximation methodology described in Secs. III and IV is evaluated for networks with different types of distributions for conductances by comparison against numerical simulation results. For convenience, we abbreviate the overall methodology as NEMA-DCA (nonuniform effective medium approximation and diffusional continuum approximation). As a further point of comparison, a more direct application of the diffusional approximation is given, in which each conductance is first replaced by its mean or expected value—this is precisely the simplified approach suggested at the very beginning of Sec. III; we term this approach the averaged diffusional approximation (ADA). Note that the use of the effective medium approximation by itself (i.e., without a continuum approximation) does not directly yield useful results, since the resulting transport equations are not less complex than the original master equation.

To simplify the mathematics, we consider cases where the conductances do not vary with space or direction, but have different probability distributions with respect to the throat length. Three characteristic types are considered for the distribution of nonzero conductances within the medium: (1) a single, discrete value (Sec. V D); (2) a continuous distribution

of conductances (Sec. V E); for comparison, this distribution is chosen to have the same shape as in the previous case, but independently of throat length; and (3) conductances inversely proportional to throat length (Sec. V F).

A. Simulation parameters

To simplify the calculations, the pore networks are considered to be contained within an n-dimensional cube having side length w, in which the pores are independently distributed with a uniform distribution. The number of pores is set to $N = 10\,000$, and the pores are assumed to be identical in terms of their additional properties $\boldsymbol{\xi}$, resulting in all pores having the same volume, V_0. As such, the extended space can be considered to consist of only the spatial dimensions $\mathbf{y} = \mathbf{x}$. Consequently, the pore network is contained within a hypercube of n volume w^n, and within this cube $f(\mathbf{x}) \equiv w^{-n}$, resulting in constant porosity

$$\phi(\mathbf{y}) = \phi_0 = N V_0 / w^n. \qquad (30)$$

For further simplification, we consider a case where the probability distribution for the conductance of a throat is determined only by the quantity $r_{ij} = ||\mathbf{x}_i - \mathbf{x}_j||$, which is the distance between the pores—this is directly related to the throat length, though in general they are not equal since the pores are not single points and the throats may be curved. Consequently, $f(g \mid \mathbf{x}_i, \mathbf{x}_j) = f(g \mid r_{ij})$ and $\tilde{g}_2(\Delta \mathbf{x}, 2\mathbf{x}) = \tilde{g}(r)$. As a result of this, the simulated networks can be described by a single diffusion coefficient which is independent of position and orientation—that is, they are homogeneous and isotropic with respect to macroscopic diffusivity.

In order to localize the connections within the medium, we define the throat probability function as a rectangular function of the interpore distance,

$$\Psi(r) = \begin{cases} 0, & \text{if } r > r_m \\ p, & \text{if } r \leqslant r_m. \end{cases} \qquad (31)$$

From Eq. (6), we can see that the expected coordination number for any given pore is independent of its location, and takes the form

$$z = \frac{p N K_n}{w^n} \int_0^{r_m} r^{n-1} \, dr = \frac{p N K_n r_m^n}{n w^n}, \qquad (32)$$

where K_n is the "surface area" of an n sphere of unit radius. For convenience, we select as a characteristic distance r_0 the root mean squared distance between connected pores in the effective medium, which in this case is described by the equation

$$\frac{r_0^2}{n} = \frac{r_m^2}{n+2}. \qquad (33)$$

B. Analytical methods

Given the simulation parameters above, application of the EMA described in Sec. III results in a new network whose average coordination number is $\tilde{z} = z/p$, with no throats connecting pores further than r_m apart, i.e., $\tilde{g}(r) = 0$ for $r > r_m$. On the other hand, for $r \leqslant r_m$, there is a single value of $\tilde{h}_{\text{in}}$ that is constant throughout the medium, and Eq. (15)

takes the form

$$\frac{1}{N-1} = \int_0^\infty \frac{f(g)}{2 + \tilde{h}_{\text{in}}/g} \, dg. \tag{34}$$

For $r \leqslant r_m$, we have $\tilde{h} = \tilde{h}_{\text{in}}/2$ and so Eq. (9) takes the form

$$\tilde{g}(r) = \int_0^\infty \frac{f(g \mid r)}{1/g + 2/\tilde{h}_{\text{in}}} \, dg, \tag{35}$$

while the diffusional approximation of Eq. (28) takes the simplified homogeneous and isotropic form

$$\frac{\partial C}{\partial t}(\boldsymbol{x},t) = D\nabla^2 C(\boldsymbol{x},t), \tag{36}$$

in which the diffusion coefficient is

$$D = \frac{\tilde{z}}{2V_0 r_m^n} \int_0^{r_m} r^{n+1} \tilde{g}(r) \, dr. \tag{37}$$

C. Numerical method

In order to calculate numerical results for comparison with the derived equations, a relatively simple approach has been used. The graph is constructed as a symmetric $N \times N$ sparse matrix, in typical fashion for a weighted graph—throat conductances are represented by the nonzero values. In a modified form, this matrix can represent the master equation for every pore in the system as a matrix equation, which can be solved subject to appropriate boundary conditions.

In these examples, steady-state solutions to the master equation are considered, in which the boundary conditions are specified by setting pores on opposing sides—specifically, within distance ϵ of opposing faces of the cube—are fixed at different levels of concentration, and the resulting flow rate Q is calculated using the aforementioned matrix method. This allows simulated diffusion coefficients to be calculated as

$$D_{\text{sim}} = \frac{Qw(w - 2\epsilon)}{N V_0 \Delta C}, \tag{38}$$

where ΔC is the difference in concentration between the two sides.

The following sections will compare the numerically derived diffusion coefficients to analytical results using ADA (labeled as D_a) and using NEMA-DCA (D_{em}). In order to display the nontrivial dependence of the diffusion coefficients on z, the diffusion coefficients shown in the figures are normalized to the dimensionless form

$$\hat{D} = D \frac{n V_0}{g_0 r_0^2}, \tag{39}$$

where g_0 is a characteristic conductance value. Although g_0 is defined differently in some of the cases below, in each case the scaling factor $n V_0/g_0 r_0^2$ is the same for both the analytical and numerical methods.

D. Single-valued distribution

In this case, a class of networks is evaluated in which the conductance values, when present, always have a fixed conductance value, g_0. As stated previously, each throat has probability $p = z/\tilde{z}$ of being present if the distance between the pores is no greater than r_m, and zero probability of being present otherwise.

Applying the ADA method would use $\bar{g}(r) = (z/\tilde{z})g_0$; implementing this instead of $\tilde{g}$ in Eq. (37) predicts a diffusion coefficient of

$$D_a = \frac{z}{2} \frac{g_0 r_0^2}{n V_0}. \tag{40}$$

On the other hand, for the NEMA-DCA method, Eq. (34) gives

$$\tilde{h}_{\text{in}} = g_0(z - 2). \tag{41}$$

Applying Eq. (35) for $r \leqslant r_m$ leads to

$$\tilde{g}(r) = \frac{z-2}{\tilde{z}} g_0, \tag{42}$$

which, when used in Eq. (37), gives

$$D_{\text{em}} = \frac{z-2}{2} \frac{g_0 r_0^2}{n V_0}. \tag{43}$$

A comparison of simulation results in 1, 2, and 3 dimensions to the predicted diffusion coefficients for the single-valued conductance distribution is given in Fig. 1. Note that the axes, z and $\hat{D}$, are both dimensionless. The graph demonstrates the accuracy of NEMA-DCA for varying numbers of physical dimensions, n, and varying values of z. While ADA predicts the asymptotic behavior as $z \to \infty$, its relative error is rather high at lower values of z. On the other hand, NEMA-DCA performs quite well for $z \gtrsim 2$. Nonetheless, neither approach correctly predicts the behavior near the percolation limit, nor the percolation limit itself—this is to be expected, as EMA methodologies in general fail in approximating percolation.

Although our networks take an irregular form, the results shown in Fig. 1 are quite similar to those for Kirkpatrick's simple regular network [15]. The predictions of NEMA-DCA reflect the tendency for low coordination numbers to significantly reduce transport coefficients in physical porous media, as compared to the predictions of a simple diffusional approximation.
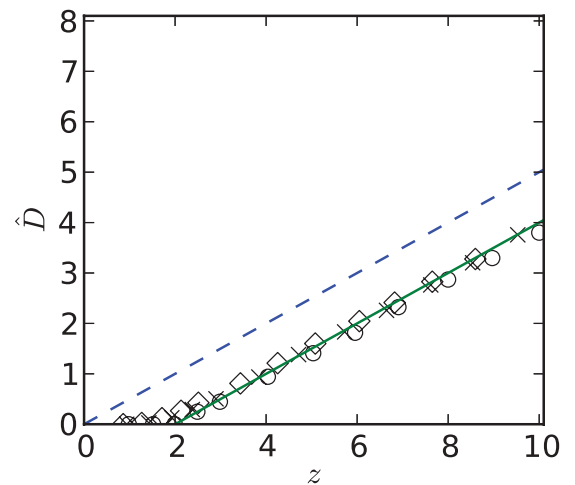

FIG. 1. (Color online) Results for the single-valued conductance distribution. The circle, cross, and diamond markers are the results of simulations for $n = 1$, $n = 2$, and $n = 3$, respectively, the dashed line is derived from ADA, and the solid line is derived from NEMA-DCA.

E. Distance-independent inverse distribution

As before, we consider $n = 1$, with no throats for pores further than r_m apart, while throats covering shorter distances have a fixed probability $z/\bar{z}$ of being present. However, in this case, when a throat is present its conductance is determined (independently of r) by the distribution

$$f_G^*(g) = \frac{k}{r_m} g^2, \qquad (44)$$

where k is a constant. As mentioned earlier, the star superscript indicates that this distribution is conditional on a throat actually being present, i.e., $G > 0$. For this example, we define the characteristic conductance as $g_0 = k/r_0$. Notably, ADA would fail entirely in this case, as $\bar{g} = \infty$ and so,

$$D_a = \infty. \qquad (45)$$

However, the application of NEMA removes this singularity. By using Eq. (44) in Eq. (34), we get

$$\frac{r_m}{kz} = \int_{k/r_m}^{\infty} \frac{1}{2g^2 + \tilde{h}_{\text{in}} g} \, dg. \qquad (46)$$

If we define the function B implicitly by

$$1 + B(s) = \exp\left(\frac{2B(s)}{s}\right), \qquad (47)$$

then $\tilde{h}_{\text{in}}$ can be expressed as $\tilde{h}_{\text{in}} = 2kB(z)/r_m$.

However, in this case Eq. (35) becomes

$$\tilde{g}(r) = \frac{2kB(z)}{r_m \tilde{z}}, \qquad (48)$$

for $r \leqslant r_m$. Note that, as in the single-valued case, this value does not depend on r, and so every throat in the effective medium has the same conductance.

Using Eq. (48) in Eq. (37) we derive the diffusion coefficient

$$D_{\text{em}} = \frac{B(z)}{\sqrt{3}} \frac{g_0 r_0^2}{V_0}. \qquad (49)$$

A comparison of simulation results to the predicted diffusion coefficients for the distance-independent inverse conductance distribution is given in Fig. 2. Once again, NEMA-DCA performs quite well, though it does not predict the percolation threshold accurately. On the other hand, ADA in this case is only valid for infinite z, as it predicts infinite diffusion coefficients.

Although this example presents an extreme case, it serves to illustrate the use of effective medium techniques in order to provide a realistic account for the effects of sparse high-throughput connections within irregular porous media. Such connections can be present in physical porous media, but it is clear that the overall throughput would nonetheless be bottlenecked by the smaller connections, as is predicted by NEMA-DCA for lower values of z.

F. Inverse-distance distribution

For this example, we once again have throats being present with probability $z/\bar{z}$ if $r \leqslant r_m$, and as in the previous example we select $n = 1$. However, in this case, whenever such a throat is indeed present, its conductance takes the value $g = k/r$.
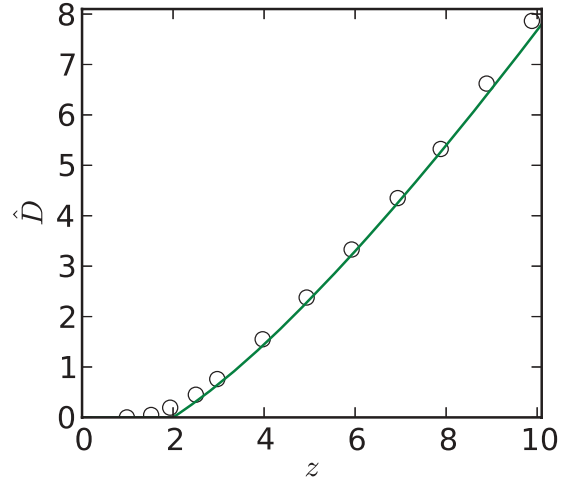

FIG. 2. (Color online) Results for the distance-independent inverse conductance distribution, all for $n = 1$. The circle markers are simulation results, while the solid line is derived from NEMA-DCA. No line is shown for ADA, as it predicts infinite coefficients in this case.

For simplicity and ease of comparison to the previous case, we define the characteristic conductance as $g_0 = k/r_0$.

In this case, the ADA approach would use $\bar{g}(r) = (z/\bar{z})(k/r)$, which when used in Eq. (37) gives

$$D_a = \frac{\sqrt{3}z}{4} \frac{g_0 r_0^2}{V_0}. \qquad (50)$$

To apply NEMA-DCA, we require a PDF for the conductances. Since $f^*(r) = 1/r_m$, it follows that

$$f^*(g) = \frac{k}{r_m} g^2. \qquad (51)$$

Notably, this is, in fact, the same distribution of conductances as in the previous example, and the interpore distances r also retain the same distribution as before, but this case is quite different from the previous one due to the correlation between the conductance and interpore distance. Consequently, if the dependence of conductance on distance were ignored, NEMA-DCA would make the same prediction here as in the previous case.

Since the conductance distribution is the same, Eq. (34) takes an identical form to that in the previous case, and so once again we have $\tilde{h}_{\text{in}} = 2kB(z)/r_m$, while the function $B(z)$ is determined by Eq. (47). With Eq. (35) for $r \leqslant r_m$ this gives

$$\tilde{g}(r) = \frac{z/\tilde{z}}{r/k + r_m/[kB(z)]}, \qquad (52)$$

and, from Eq. (37),

$$\begin{aligned} D_{\text{em}} &= \frac{kz}{2V_0 r_m} \int_0^{r_m} \frac{r^2}{r + r_m/B(z)} \, dr \\ &= \frac{\sqrt{3}}{4} \left[z - 2\frac{z-2}{B(z)} \right] \frac{g_0 r_0^2}{V_0}. \end{aligned} \qquad (53)$$

A comparison of simulation results to the predicted diffusion coefficients for the inverse-distance conductance distribution is given in Fig. 3. As can be seen, NEMA-DCA is very accurate except near the percolation limit, while ADA
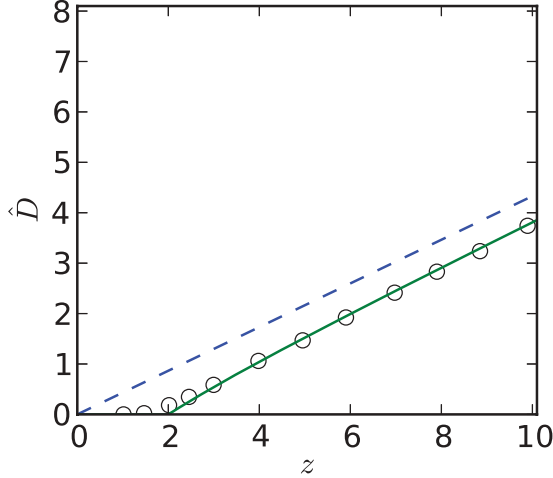
FIG. 3. (Color online) Results for the inverse-distance conductance distribution, all for $n = 1$. The circle markers are simulation results, the dashed line is derived from ADA, and the solid line is derived from NEMA-DCA.

predicts the asymptotic behavior and is accurate only for larger z. Like the first example, this example illustrates the need to account for the effects of limited interconnectedness in order to achieve a realistic model.

G. Overall discussion

In contrasting the last two cases, with differing inverse distributions, it is clear from Figs. 2 and 3 that the results are very different—the radius-independent distribution gives a higher diffusion coefficient by a factor of 2 at $z = 10$, and it is clear from the shape of the curve that this divergence persists for increasing z. This shows the importance of properly representing various property correlations, especially between pores and throats, in the porous medium. Such correlations are the only difference between the cases in Figs. 2 and 3, and it is clear that these kinds of correlations are an essential aspect of real-world porous media. Unlike NEMA, a more typical EMA (e.g., Kirkpatrick [15]) would not be able to account for this type of behavior.

However, it is interesting to note that in each case, the NEMA predicts a percolation limit at $z = 2$, just as in Kirkpatrick's paper [15]—this seems to be a universal property of single-bond effective medium approximations, regardless of whether the network in question is regular or irregular in nature. Notably, as is demonstrated by the second example, the behavior away from $z = 2$ does not need to be linear. Although the numerical results show that the behavior very close to the true percolation limit is not correctly predicted, as is generally the case for effective medium approximations, it can be seen that the NEMA-DCA prediction starts to match the numerical results very closely at a short distance from the percolation limit.

Moreover, the general interdisciplinary tool developed in this paper can be applied to Fickian diffusion, Knudsen diffusion, and incompressible Newtonian Stokes flow; example throat conductance expressions for some simple throat geometries are presented in Table I of Appendix A.

TABLE I. Expressions for throat conductance g for various transport phenomena. Where applicable, a is the radius of the throat, L is the length of the throat, D is the diffusion coefficient, $\bar{v}$ is the mean molecular speed, μ is the fluid viscosity, and σ is the electrical conductivity of the material.

	Expression for g		
Case	Small orifices $(L = 0)$	Long, narrow throats $(L \gg a)$	Ref.
A	$2Da$	$D\pi a^2/L$	[38]
B	$\bar{v}\pi a^2/4$	$2\bar{v}\pi a^3/(3L)$	[39]
C	$a^3/(3\mu)$	$\pi a^4/(8\mu L)$	[40]
D		$\sigma\pi a^2/L$	

VI. CONCLUSIONS

In this paper, we have presented a general analytical methodology for analyzing various transport phenomena in irregular porous media. We have developed a generalized effective medium approximation which allows the conductances of the throats in the medium to vary depending on the properties and positions of the pores they connect. This is used in combination with a continuum approximation in the form of a diffusionlike equation to derive an explicit analytical expression for the transport coefficients, allowing for an efficient model of transport that retains the ability to account for microscopic effects.

These analytical expressions have been tested against several numerical simulations with different types of distributions for throat properties, demonstrating very good accuracy for the proposed methodology, except in the vicinity of the percolation limit. Furthermore, the results demonstrate the ability of this method to account for several physical effects, including reduced transport due to low coordination numbers, and the effects of correlations between local properties of the medium.

APPENDIX A: EXPRESSIONS FOR THROAT CONDUCTANCES

Recalling that the master equation

$$\frac{dm_i}{dt} = \sum_{j=1}^{N} q_{ji} = \sum_{j=1}^{N} g_{ij}(c_j - c_i) \tag{A1}$$

applies to a variety of different types of transport, Table I gives examples of throat conductances for a variety of different cases.

The cases considered in Table I are (A) *Fickian diffusion*. (B) *Knudsen diffusion*. (C) *Incompressible Newtonian Stokes flow*. Since the flow is steady, there is no time derivative term; c_i is interpreted as the pressure in each pore, while q_{ij} is the volumetric flow rate through the throat from pore i to pore j. (D) *Flow of electrical current*. Once again, the flow is

steady; c_i is the voltage at node (pore) i, and q_{ij} is the current flowing through the branch (throat) from node i to node j. Note that in the case of electrical transport, the "pores" and "throats" usually consist of the solid matrix rather than the void space.

APPENDIX B: APPROXIMATION FOR $\tilde{g}$

Starting with the effective medium criterion [Eq. (8)],

$$\int_0^\infty f(g \mid \boldsymbol{y}_i, \boldsymbol{y}_j) \frac{g - \tilde{g}(\boldsymbol{y}_i, \boldsymbol{y}_j)}{g + \tilde{h}(\boldsymbol{y}_i, \boldsymbol{y}_j)} \, dg = 0, \qquad \text{(B1)}$$

we apply Eq. (2), resulting in

$$(1 - \Psi) \frac{\tilde{g}}{\tilde{h}} = \Psi \int_0^\infty f^*(g \mid \boldsymbol{y}_i, \boldsymbol{y}_j) \frac{g - \tilde{g}}{g + \tilde{h}} \, dg, \qquad \text{(B2)}$$

where Ψ, $\tilde{g}$, and $\tilde{h}$ are, as before, functions of $\boldsymbol{y}_i$ and $\boldsymbol{y}_j$—the arguments have been dropped for compactness. This can be rearranged to give

$$\tilde{g} = \frac{\Psi}{\chi} \int_0^\infty \frac{f^*(g \mid \boldsymbol{y}_i, \boldsymbol{y}_j)}{1/g + 1/\tilde{h}} \, dg, \qquad \text{(B3)}$$

where

$$\chi = 1 - \Psi \left[1 - \int_0^\infty \frac{f^*(g \mid \boldsymbol{y}_i, \boldsymbol{y}_j)}{1 + g/\tilde{h}} \, dg \right]. \qquad \text{(B4)}$$

Since f^* is a PDF and the conductances must take positive values, the integral within the brackets is bounded below by 0 and above by 1, and so $1 - \Psi \leqslant \chi \leqslant 1$. For $\Psi \ll 1$, we get $\chi \sim 1$ and hence Eq. (B3) can be written as

$$\tilde{g}(\boldsymbol{y}_i, \boldsymbol{y}_j) = \int_0^\infty \frac{f(g \mid \boldsymbol{y}_i, \boldsymbol{y}_j)}{1/g + 1/\tilde{h}(\boldsymbol{y}_i, \boldsymbol{y}_j)} \, dg, \qquad \text{(B5)}$$

since the $\delta(g)$ component of the integral vanishes due to the $1/g$ term in the denominator. This completes the derivation of Eq. (9).

APPENDIX C: DERIVATION OF THE DIFFUSIONAL APPROXIMATION

Based on the assumption in Sec. III that the network has no long-range connectivity and its statistical properties do not change significantly within any locale, we expect that power

series expansions should offer reasonable approximations for f and $\tilde{g}_2$, and, based on the form of Eq. (26), for C. The power series expansions for $C(\boldsymbol{y} + \Delta\boldsymbol{y}, t) - C(\boldsymbol{y}, t)$, $f(\boldsymbol{y} + \Delta\boldsymbol{y})$, and $\tilde{g}_2(\Delta\boldsymbol{y}, \boldsymbol{y} + \Delta\boldsymbol{y})$, are as follows:

$$C(\boldsymbol{y} + \Delta\boldsymbol{y}, t) - C(\boldsymbol{y}, t)$$
$$= \Delta y^\alpha \frac{\partial C}{\partial y^\alpha}(\boldsymbol{y}, t) + \frac{1}{2} \Delta y^\alpha \Delta y^\beta \frac{\partial^2 C}{\partial y^\alpha \partial y^\beta}(\boldsymbol{y}, t) + \cdots, \quad \text{(C1)}$$

$$f(\boldsymbol{y} + \Delta\boldsymbol{y}) = f(\boldsymbol{y}) + \Delta y^\alpha \frac{\partial f}{\partial y^\alpha}(\boldsymbol{y}) + \cdots, \qquad \text{(C2)}$$

and

$$\tilde{g}_2(\Delta\boldsymbol{y}, 2\boldsymbol{y} + \Delta\boldsymbol{y}) = \tilde{g}_2(\Delta\boldsymbol{y}, 2\boldsymbol{y}) + \frac{1}{2} \Delta y^\alpha \frac{\partial \tilde{g}_2}{\partial y^\alpha}(\Delta\boldsymbol{y}, 2\boldsymbol{y}) + \cdots.$$
$$\text{(C3)}$$

Using these expansions while discarding third- and fourth-order terms allows the reduced master equation to be expressed as

$$\frac{\partial M}{\partial t} = \frac{N^2}{2} \int_S \Delta y^\alpha \Delta y^\beta \left(f^2 \tilde{g}_2 \frac{\partial^2 C}{\partial y^\alpha \partial y^\beta} + f^2 \frac{\partial \tilde{g}_2}{\partial y^\alpha} \frac{\partial C}{\partial y^\beta} \right.$$
$$\left. + 2f \frac{\partial f}{\partial y^\alpha} \tilde{g}_2 \frac{\partial C}{\partial y^\beta} \right) d(\Delta\boldsymbol{y}), \qquad \text{(C4)}$$

where the arguments for the functions are dropped for compactness; as before, f and its derivatives are evaluated at $\boldsymbol{y}$, $\tilde{g}_2$ and its derivatives are evaluated at $(\Delta\boldsymbol{y}, 2\boldsymbol{y})$, and C and its derivatives are evaluated at $(\boldsymbol{y}, t)$.

Note that the first-order (drift) terms in this equation are zero. This follows from the fact that $f(\boldsymbol{y})$ and $C(\boldsymbol{y}, t)$ are independent of $\Delta\boldsymbol{y}$, while g_2 is even with respect to $\Delta\boldsymbol{y}$, resulting in

$$\int_S \Delta y^\alpha \tilde{g}_2 \, d(\Delta\boldsymbol{y}) = 0. \qquad \text{(C5)}$$

Using the product rule, as well as the aforementioned independence, Eq. (C4) can be expressed as

$$\frac{\partial M}{\partial t} = \frac{\partial}{\partial y^\alpha} \left[\frac{N^2}{2} f^2 \int_S \Delta y^\alpha \Delta y^\beta \tilde{g}_2 \, d(\Delta\boldsymbol{y}) \frac{\partial C}{\partial y^\beta} \right], \quad \text{(C6)}$$

completing the derivation of the diffusional approximation.

[1] A. Tamayol and M. Bahrami, J. Power Sources **196**, 3559 (2011).

[2] G. Truskey, F. Yuan, and D. Katz, *Transport Phenomena in Biological Systems*, Pearson Prentice Hall Bioengineering (Prentice Hall, Upper Saddle River, NJ, 2009).

[3] M. Odabaee and K. Hooman, Appl. Therm. Eng. **36**, 456 (2012).

[4] C. T'Joen, P. D. Jaeger, H. Huisseune, S. V. Herzeele, N. Vorst, and M. D. Paepe, Int. J. Heat Mass Transf. **53**, 3262 (2010).

[5] A. Bejan, I. Dincer, S. Lorente, A. Miguel, and A. Reis, *Porous and Complex Flow Structures in Modern Technologies* (Springer, New York, 2004).

[6] A. Bejan and A. M. Morega, J. Heat Transfer **115**, 75 (1993).

[7] K. Hooman and H. Gurgenci, Transp. Porous Media **84**, 257 (2010).

[8] S. Whitaker, *The Method of Volume Averaging*, Theory and Applications of Transport in Porous Media (Kluwer, Dordrecht, 1999).

[9] A. Klimenko, D. Saulov, P. Massarotto, and V. Rudolph, Transp. Porous Media **92**, 745 (2012).

[10] A. S. Al-Kharusi and M. J. Blunt, J. Petrol. Sci. Eng. **56**, 219 (2007).

[11] A. Tamayol and M. Bahrami, Phys. Rev. E **83**, 046314 (2011).

[12] M. Sahimi, Phys. Rev. E **85**, 016316 (2012).

[13] S. Fedotov, S. Kim, and H. Pitsch, *Anomalous Knudsen Diffusion and Reactions in Disordered Porous Media*, Annual Research Briefs (Center for Turbulence Research, Stanford, CA, 2007).

[14] B. Berkowitz, A. Cortis, M. Dentz, and H. Scher, Rev. Geophys. **44**, RG2003 (2006).

[15] S. Kirkpatrick, Rev. Mod. Phys. **45**, 574 (1973).

[16] V. N. Burganos and S. V. Sotirchos, AlChE J. **33**, 1678 (1987).

[17] R. Jackson, *Transport in Porous Catalysts*, Chemical Engineering Monographs (Elsevier, Amsterdam, 1977).

[18] J. Koplik, J. Phys. C: Solid State Phys. **14**, 4821 (1981).

[19] J. Bernasconi, Phys. Rev. B **9**, 4575 (1974).

[20] P. G. Toledo, H. Davis, and L. Scriven, Chem. Eng. Sci. **47**, 391 (1992).

[21] S. Mukhopadhyay and M. Sahimi, Chem. Eng. Sci. **55**, 4495 (2000).

[22] N. A. Vrettos, H. Imakoma, and M. Okazaki, J. Appl. Phys. **66**, 2873 (1989).

[23] M. Sahimi and T. T. Tsotsis, Ind. Eng. Chem. Res. **36**, 3043 (1997).

[24] J. Dall and M. Christensen, Phys. Rev. E **66**, 016121 (2002).

[25] V. D. P. Servedio, G. Caldarelli, and P. Buttà, Phys. Rev. E **70**, 056126 (2004).

[26] P. Bedrikovetsky, *Mathematical Theory of Oil and Gas Recovery: With Applications to Ex-USSR Oil and Gas Fields*, Petroleum Engineering and Development Studies (Kluwer, Dordrecht, The Netherlands, 1993).

[27] A. Hunt and R. Ewing, *Percolation Theory for Flow in Porous Media*, Lecture Notes in Physics (Springer, Berlin, 2009).

[28] H. Dong and M. J. Blunt, Phys. Rev. E **80**, 036307 (2009).

[29] P. Øren and S. Bakke, J. Petrol. Sci. Eng. **39**, 177 (2003).

[30] A. Sheppard, R. Sok, and H. Averdunk, in International Symposium of the Society of Core Analysts, Toronto, Canada, 2005 (unpublished).

[31] R. Al-Raoush and C. Willson, J. Hydrol. **300**, 44 (2005).

[32] Z. Jiang, K. Wu, G. Couples, M. Van Dijke, K. Sorbie, and J. Ma, Water Resour. Res. **43**, W12S03 (2007).

[33] Note that in our terminology z is the mean coordination number of the stochastic network, while Kirkpatrick's z is equivalent to our $\tilde{z}$. In this simple example $\tilde{z} = z/p$.

[34] I. G. Vladimirov and A. Y. Klimenko, Multiscale Model. Simul. **8**, 1178 (2010).

[35] M. Sahimi, B. D. Hughes, L. E. Scriven, and H. T. Davis, J. Chem. Phys. **78**, 6849 (1983).

[36] J. Cserti, Am. J. Phys **68**, 896 (2000).

[37] As a visual aid, consider the case of two spheres of equal radius in three dimensions, with the center of each sphere being located within the other; in this case, the overlap between the spheres is at least 5/16 of the volume of either sphere.

[38] L. Dagdug, A. M. Berezhkovskii, S. Y. Shvartsman, and G. H. Weiss, J. Chem. Phys. **119**, 12473 (2003).

[39] R. Present, *Kinetic Theory of Gases* (McGraw-Hill, New York, 1958).

[40] H. L. Weissberg, Phys. Fluids **5**, 1033 (1962).